Journal of Pressure Vessel Technology. December 22, 2024;
Accepted manuscript posted September 19, 2025. 10.1115/1.4069837
Copyright (c) 2024 by ASME

Check for updates

Investigative studies on various metal loss flaws and their progression from a deep pinhole size to a lengthy size in pressurized tubes

Ifeanyi E. Kalu[1,2], Helen M. Inglis[1], Schalk Kok[1]

[1]Centre for Asset Integrity Management, Department of Mechanical and Aeronautical Engineering, University of Pretoria, Private Bag X20, Hatfield, Pretoria 0028, South Africa.

[2]Physics Advanced Research Centre, Sheda Science and Technology Complex (SHESTCO), P.M.B 186, Garki, Abuja, Nigeria.

Accepted Manuscript Not Copyedited

Abstract

Localized metal loss (LML) in pressurized tubes is a primary contributor to tube failures and unplanned shutdowns and in industrial boilers. Initially, these tubes may have inconspicuous anomalies introduced during manufacturing, testing, and inspection. Over time, as the vessels are deployed and exposed to harsh environmental, operating, or aging conditions, these anomalies evolve, eventually leading to their failure. In this paper, detailed investigative studies on various metal loss flaws were carried out to acquire insights on their failure behaviour and mechanism, especially as they progress from very small size to lengthy size. Three investigations were carried out to identify which geometric parameters are most critical for predicting failure of the tubes and to what extent will they influence their failure. First, a range of real flaws that failed while operating under high internal pressure in a steam boiler were considered. The study compared two different modeling methods for evolving flaws to their failure geometry. The outcome show that for most flaws, the failure evaluation is insensitive to the method of evolving the flaw to failure. Second, all the flaw geometries were modeled using the same material and operating conditions and their failure behaviour studied. The findings shows that failure pressure depends solely on the flaw thickness, and not on the other flaw dimensions, except for pinhole flaws. Finally, a range of flaw geometries, spanning the

Downloaded from http://asmedigitalcollection.asme.org/pressurevesseltech/article-pdf/doi/10.1115/1.4069837/7538655/pvt-24-1191.pdf by University of Pretoria, Ifeanyi Emmanuel Kalu on 21 September 2025

Journal of Pressure Vessel Technology. December 22, 2024;
Accepted manuscript posted September 19, 2025. 10.1115/1.4069837
Copyright (c) 2024 by ASME

space from localized pinhole flaws to wide lengthy flaws were investigated. Outcomes of these studies show that failure pressure for small flaws is sensitive to the flaw geometry. However, the failure pressure ceases to depend on the flaw length once the flaw length is greater than twice the tube diameter, and ceases to depend on the flaw width when the flaw length is greater than the tube diameter. These results suggest that gross plastic collapse is not the dominant failure mechanism for small flaws. However, for flaws with a length at least twice the tube diameter, the flaw dimension which predicts failure is the tube remaining thickness in the deepest part of the flaw. These studies establish the applicability limits of gross plastic collapse analysis for pressurized tubes experiencing metal loss, and demonstrate opportunities for simplifying flaw analysis for sufficiently large flaws. Ultimately, the insights from this study will contribute towards appropriate preventive maintenance of these critical assets while in operation.

Keywords: Localized metal loss, pressurized tubes, flaw shapes and geometries, failure pressure, gross plastic collapse.

Accepted Manuscript Not Copyedited

Downloaded from http://asmedigitalcollection.asme.org/pressurevesseltech/article-pdf/doi/10.1115/1.4069837/7538655/pvt-24-1191.pdf by University of Pretoria, Ifeanyi Emmanuel Kalu on 21 September 2025

Journal of Pressure Vessel Technology. December 22, 2024;
Accepted manuscript posted September 19, 2025. 10.1115/1.4069837
Copyright (c) 2024 by ASME

1 Introduction

Pressure vessels such as boiler tubes and pipes used in process, manufacturing, power and nuclear plants are prone to various in-service failure issues. This is due to the harsh environment or conditions (particularly high pressure and high temperature) which they are subjected to while in use. Metal loss resulting from manufacturing flaws or in-service mechanical damage, erosion and corrosion is one significant contributor to failures. This may take the form of general or localized metal loss on the exterior or interior part of the vessel. Localized metal loss (LML), particularly influenced by internal/external pressure and erosive or corrosive substances impinging on the exterior surface of pressurized vessels over time, can result in wall thinning and ultimately failure of these vessels. This is well illustrated by the case of erosion caused by fly ash in boiler tubes, which leads to the failure of the tubes at operating conditions that vary from their design conditions [1], often driven by plastic deformation. For the case of external LML, yielding begins at the thinnest portion of the flaw, extending from the outer diameter to the inner diameter of the tube and can lead to in-service failure of the tubes by gross plastic collapse. This is a frequent cause of unplanned boiler outages in industrial plants [1–3], leading to loss in production [2–4], expensive emergency repairs [3] and, by implication, increased maintenance costs.

Efforts have been made over the years to mitigate this problem of metal loss on pressurized tubes. These include: prediction of a boiler tube remaining life based on a reference failure stress and the tube geometry [5–7], time to failure prediction of tubes in service using various stress and strain limits [7], estimation of the burst failure or plastic collapse for localized pits or scars [8–10], provision of guidelines to regulate erosive particles impinging on the tubes and the use of screens to redirect the particles, minimize erosion rates and velocities of the flue gases [4,11]. Failure benchmarks have been recommended to guide against collapse of the pressure vessels while in service, such as using a plastic strain limit of 2% [12–14] or a stress

Accepted Manuscript Not Copyedited

Downloaded from http://asmedigitalcollection.asme.org/pressurevesseltech/article-pdf/doi/10.1115/1.4069837/7538655/pvt-24-1191.pdf by University of Pretoria, Ifeanyi Emmanuel Kalu on 21 September 2025

Journal of Pressure Vessel Technology. December 22, 2024;
Accepted manuscript posted September 19, 2025. 10.1115/1.4069837
Copyright (c) 2024 by ASME

limit that corresponds with the flow strength or ultimate tensile strength (σ_{uts}) of the pressure vessel [15–17]. Finite element analysis (FEA) has been used to assess and evaluate tubes with localized thinning against failure [8,18–20]. This has been recommended as an efficient method of evaluating metal loss failures in pressure vessels by the American Petroleum Institute (API) and the American Society of Mechanical Engineers (ASME) [21,22]. Based on its efficacy, the FEA approach has been recommended for use when assessing ageing pressure vessels or those in prolonged service [23].

Despite efforts to address metal loss failures, they remain a significant concern, particularly in the management of ageing infrastructures within a constrained economic environment. The complexities surrounding these defects mean that more research is needed to gain deeper insight into the failure behaviour of localized flaws in pressurized vessels during operation. Investigating the tube geometry and flaw parameters that most critically influence vessel failure is also essential. To advance understanding of the failure behaviour of localized flaws in pressurized vessels during service, three comprehensive investigations were undertaken. First, the evolution of the flaw geometry from an initial flaw to the final failed dimensions was explored. To answer the question: "*Does the flaw evolution assumption influence predicted failures?"*, the case in which flaw depth increases while other flaw dimensions remain the same was compared with the scenario in which all the flaw dimensions increase proportionally. Second, the material model and tube dimensions as variables were removed from the study, remodeling all the flaws on a single tube with fixed material and dimensions. This allows us to answer the question: *"How does flaw geometry affect failure pressure?"* Finally, the failure pressures for tubes with hypothetical flaws spanning the space from short to long and from slender to wide were systematically investigated to better understand the failure behaviour of the progression of the flaws from a pinhole size to a lengthy size. The study also helps to answer the question, *"For which flaw dimensions is plastic collapse the appropriate failure model?"*

Accepted Manuscript Not Copyedited

Downloaded from http://asmedigitalcollection.asme.org/pressurevesseltech/article-pdf/doi/10.1115/1.4069837/7538655/pvt-24-1191.pdf by University of Pretoria, Ifeanyi Emmanuel Kalu on 21 September 2025

Journal of Pressure Vessel Technology. December 22, 2024;
Accepted manuscript posted September 19, 2025. 10.1115/1.4069837
Copyright (c) 2024 by ASME

Overall, the study outcomes enable the identification of distinct flaw categories that fail in fundamentally different ways. The research provides insight into the geometric parameters that define each category and their implications on tube failure during operation. Furthermore, the findings from this study will enhance our understanding of the applicability limits of gross plastic collapse analysis for pressure vessels experiencing metal loss. The study also sheds light on the extent to which flaw geometry influences the failure of these pressure vessels. Consequently, these insights will contribute to the development of effective preventive maintenance strategies for these critical assets during operation.

2 Modeling and evaluation methodology

The evaluation procedure used for all the investigations is summarized in the flow chart in Fig. 1 and described in this section. This finite element analysis procedure has been implicitly validated against data from real failed tubes [19].

2.1 Data obtained from failed tubes

A selection of failed tubes with varying flaw sizes and shapes due to localized erosion are used for this study. These tubes failed as they operated under high internal pressure in a steam boiler. Fig. 2 shows the example of a tube that failed by gross plastic collapse. Each tube is characterized by overall dimensions, flaw dimensions, material, and operating conditions. Specifically, D_o is the exterior diameter of the tube and t is the tube thickness. The flaws were measured after failure and the dimensions include t_f, the tube remaining thickness at failure, f_l and f_w, the flaw length and width, respectively. These dimensions are shown in Fig. 3. The flaw depth is calculated as $f_d = t - t_f$. The measured dimensions of the failed (effective) area in each tube are small in comparison to the entire flawed region (as seen in Fig. 2) and the tube length, so the total tube length was not recorded. The operating conditions are represented by the material operating temperature, T, and operating pressure, P.

Accepted Manuscript Not Copyedited
Downloaded from http://asmedigitalcollection.asme.org/pressurevesseltech/article-pdf/doi/10.1115/1.4069837/7538655/pvt-24-1191.pdf by University of Pretoria, Ifeanyi Emmanuel Kalu on 21 September 2025

Journal of Pressure Vessel Technology. December 22, 2024;
Accepted manuscript posted September 19, 2025. 10.1115/1.4069837
Copyright (c) 2024 by ASME

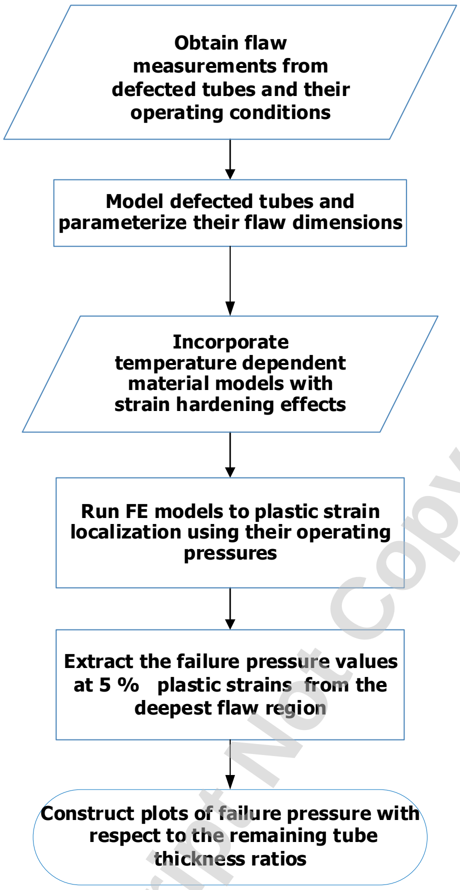

Fig. 1. Flow chart showing the assessment procedure used for the study.

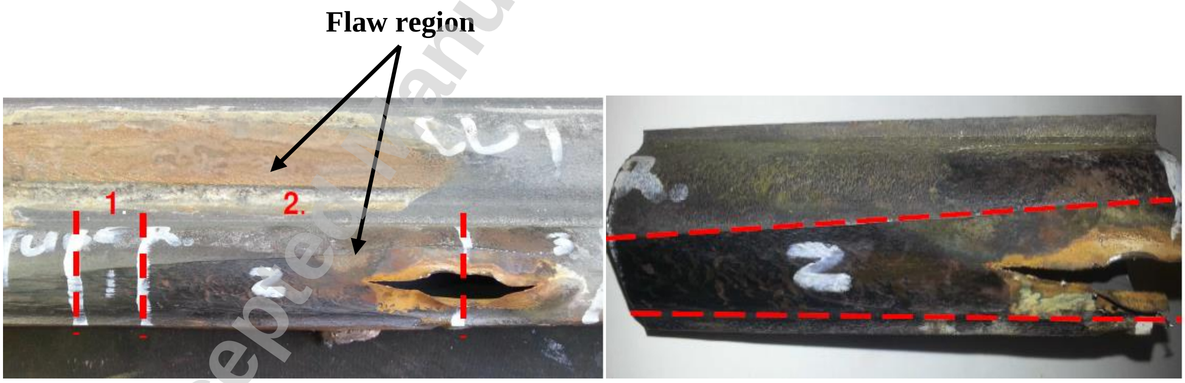

Fig. 2. A failed tube with local metal loss (left). A magnified view of the localized eroded tube (right).

The details of the five tubes examined in this research can be seen in Table 1. To enable comparison between flaws in different tubes, the flaw length and width are normalized with reference to the tube external diameter. From their normalized dimensions (f_l/D_o and f_w/Do),

Accepted Manuscript Not Copyedited

Downloaded from http://asmedigitalcollection.asme.org/pressurevesseltech/article-pdf/doi/10.1115/1.4069837/7538655/pvt-24-1191.pdf by University of Pretoria, Ifeanyi Emmanuel Kalu on 21 September 2025

Journal of Pressure Vessel Technology. December 22, 2024;
Accepted manuscript posted September 19, 2025. 10.1115/1.4069837
Copyright (c) 2024 by ASME

it can be seen that these tubes span a variety of localized metal loss (LML) scenarios, ranging from slender to wide flaws, from short to very long flaws, and including a pinhole flaw.

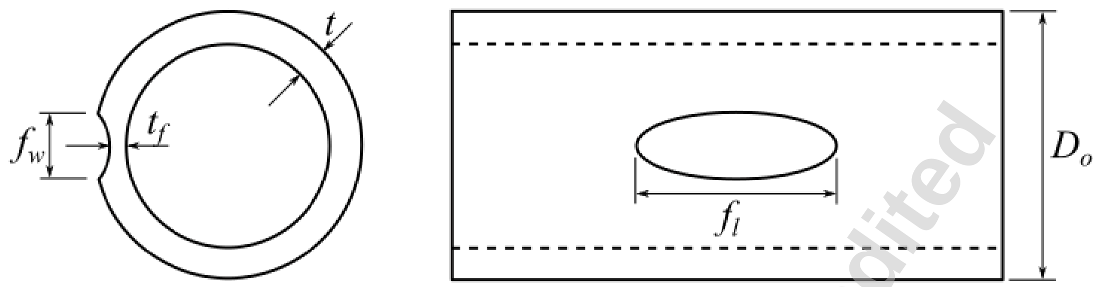

Fig. 3. Geometry of flawed tubes

Table 1. Specifications of the selected tubes, with flaw dimensions

	Tube 1	Tube 2	Tube 3	Tube 4	Tube 5
D_o (mm)	75.0	47.5	63.0	38.0	33.0
t (mm)	7.0	5.4	5.4	3.8	3.6
t_{rf} (mm)	0.50	1.20	0.42	0.45	0.20
Material	BS 3059 Grade 360	SA 210 A1	BS 3059 Grade 440	BS 3059 Grade 440	DIN 17175 15Mo3
P (MPa)	12.40	19.58	11.20	20.00	20.91
T (℃)	384	400	350	250	414
Flaw dimensions and descriptions					
f_l (mm)	600	400	310	500	20
f_w (mm)	20	45	60	35	15
f_d (mm)	6.50	4.20	4.98	3.35	3.40
f_l/D_o	8.00	8.42	4.92	13.16	0.61
f_w/Do	0.267	0.947	0.952	0.921	0.455
Flaw description	Long slender flaw	Long wide flaw	Short wide flaw	Very long wide flaw	Pinhole flaw

2.2 *Geometry and meshing*

Idealized LML flaws matching the observed flaw dimensions at failure listed in Table 1 are modelled in ANSYS® with ellipsoidal shapes, which have been considered as accurate representations of metal loss. An offset ellipse is swept over an unflawed pipe model to generate the ellipsoidal flawed shape. The geometry of the offset ellipse is calculated to match the known flaw dimensions, as described in detail in [19,20]. Fig. 4 shows the flawed tube models.

Accepted Manuscript Not Copyedited

Downloaded from http://asmedigitalcollection.asme.org/pressurevesseltech/article-pdf/doi/10.1115/1.4069837/7538655/pvt-24-1191.pdf by University of Pretoria, Ifeanyi Emmanuel Kalu on 21 September 2025

Journal of Pressure Vessel Technology. December 22, 2024;
Accepted manuscript posted September 19, 2025. 10.1115/1.4069837
Copyright (c) 2024 by ASME

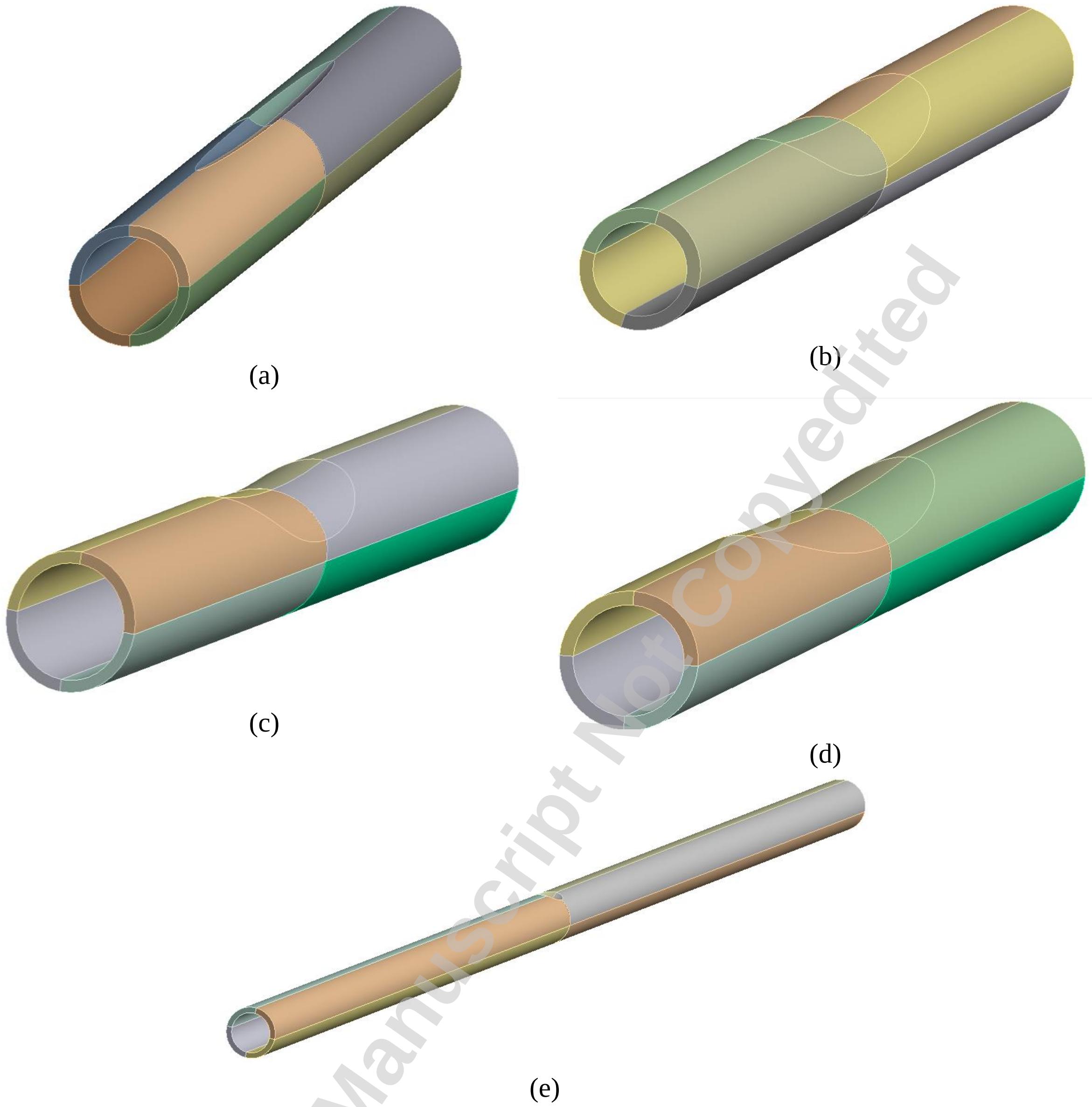

Fig. 4. Models of flawed tubes used for this study (a) Tube 1: long slender flaw (b) Tube 2: long wide flaw (c) Tube 3: short wide flaw (d) Tube 4: very long wide flaw and (e) Tube 5: pinhole flaw.

To model the effect of increasing flaw size, additional hypothetical flaws are created with varying remaining wall thickness, t_r. These additional flaws progress from an initial shallow flaw to the known final flaw dimensions. It is important to distinguish between the modeled remaining wall thickness, t_r, which changes to represent flaw evolution in the finite element analyses, and the measured remaining thickness of the tube at failure t_f.

For the analysis of the tubes, a quarter FE model that makes use of symmetry conditions is employed, as shown in Fig. 5. Along the axis of symmetry in the models, shown shaded in

Accepted Manuscript Not Copyedited

Downloaded from http://asmedigitalcollection.asme.org/pressurevesseltech/article-pdf/doi/10.1115/1.4069837/7538655/pvt-24-1191.pdf by University of Pretoria, Ifeanyi Emmanuel Kalu on 21 September 2025

Journal of Pressure Vessel Technology. December 22, 2024;
Accepted manuscript posted September 19, 2025. 10.1115/1.4069837
Copyright (c) 2024 by ASME

blue, frictionless constraints are imposed. At the model's far-left side, a remote displacement support is placed along the edges to restrict any rotational movement and displacement on the y-axis. The operating pressure, P is applied to the interior tube surface, and increased linearly with each time-step. The axial force, F, defined as a function of P, is applied at the model's far-left side, providing the corresponding axial stress without explicitly modeling end caps.

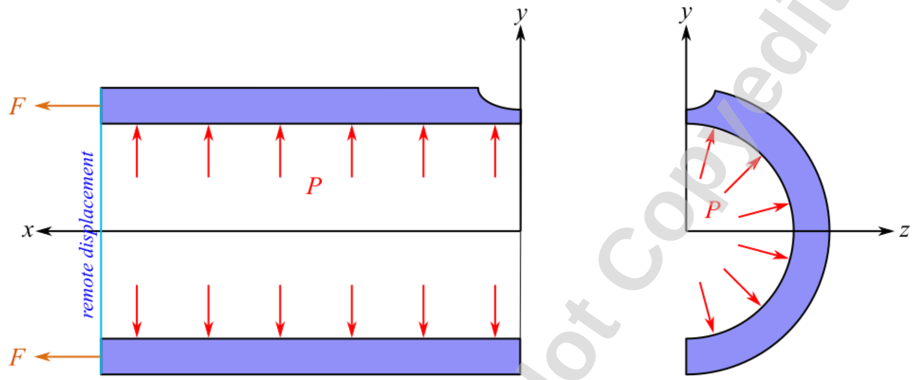

Fig. 5. Boundary conditions with operating pressure applied on the tube

The finite element mesh (shown in Fig. 6) uses predominantly quadratic hexahedral elements. Mesh quality control measures are employed locally at the flaw region to improve the mesh quality. Further refinement is performed at the tip of the flaw area, which is where the results of the analysis will be extracted, ensuring that there are a minimum of five elements through the wall thickness. The mesh quality of the models ranges from an average element quality of 0.913 with 91,804 elements for the tube with the long slender flaw to an average element quality of 0.825 with 11,793 elements for the tube having the pinhole flaw. Each model is solved on ANSYS® Mechanical platform using a step with minimum 20 sub-steps to maximum 1000 sub-steps with material nonlinear effects and large deflection active. ANSYS® direct solver type is used.

2.3 Material properties

Properties of in-service boiler tube materials are affected by the operating temperature. The temperature effect on the mechanical strength of the tubes is appropriately incorporated using the specified minimum yield strength and tensile strength based models obtained from the API

Accepted Manuscript Not Copyedited

Downloaded from http://asmedigitalcollection.asme.org/pressurevesseltech/article-pdf/doi/10.1115/1.4069837/7538655/pvt-24-1191.pdf by University of Pretoria, Ifeanyi Emmanuel Kalu on 21 September 2025

Journal of Pressure Vessel Technology. December 22, 2024;
Accepted manuscript posted September 19, 2025. 10.1115/1.4069837
Copyright (c) 2024 by ASME

579-1/ASME FFS standard [21]. The elastic modulus, E and thermal expansion coefficient, α, of the tubes at their service or operating temperature, T, are included in the study, using the BS 3059: Part 2 standard [24]. Table 2 shows the mechanical properties of the tubes at their respective in-service temperatures used for this study.

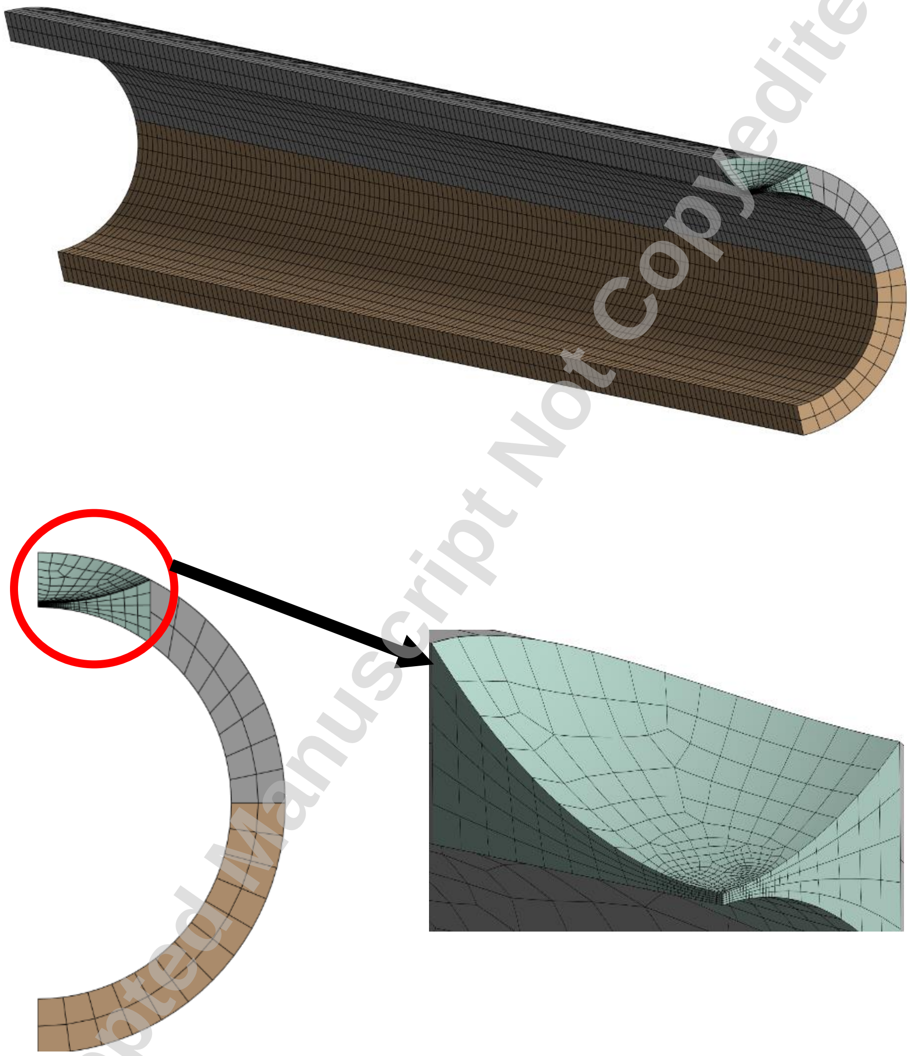

Fig. 6. One of the meshed tubes (top) with the front view (lower left) and a magnified cross-section of the well-refined flaw area (lower right).

The true stress-true strain Material Properties Council (MPC) model, referenced in the API-ASME FFS Standard, Annex 2E.3.1, [21] is adopted for this study. The material model developed for each tube, shown in Fig. 7, incorporates work hardening due to plastic deformation, as recommended by previous studies [7,23,25]. This material model is

Downloaded from http://asmedigitalcollection.asme.org/pressurevesseltech/article-pdf/doi/10.1115/1.4069837/7538655/pvt-24-1191.pdf by University of Pretoria, Ifeanyi Emmanuel Kalu on 21 September 2025

Accepted Manuscript Not Copyedited

Journal of Pressure Vessel Technology. December 22, 2024;
Accepted manuscript posted September 19, 2025. 10.1115/1.4069837
Copyright (c) 2024 by ASME

implemented in ANSYS as a multilinear isotropic hardening model that obeys von Mises associated flow plasticity theory within a large deformation framework.

Table 2. Properties of flawed tubes at their respective operating temperatures

Tubes	Temperature (℃)	σ_y (MPa)	σ_{uts} (MPa)	α ($\times 10^{-6}$ ℃$^{-1}$)	E (GPa)
Tube 1	384	170.08	260.54	13.60	184.28
Tube 2	400	181.91	296.04	13.70	183.00
Tube 3	350	182.59	327.92	13.40	187.00
Tube 4	250	197.33	354.39	12.85	194.50
Tube 5	414	240.27	400.45	13.76	181.74

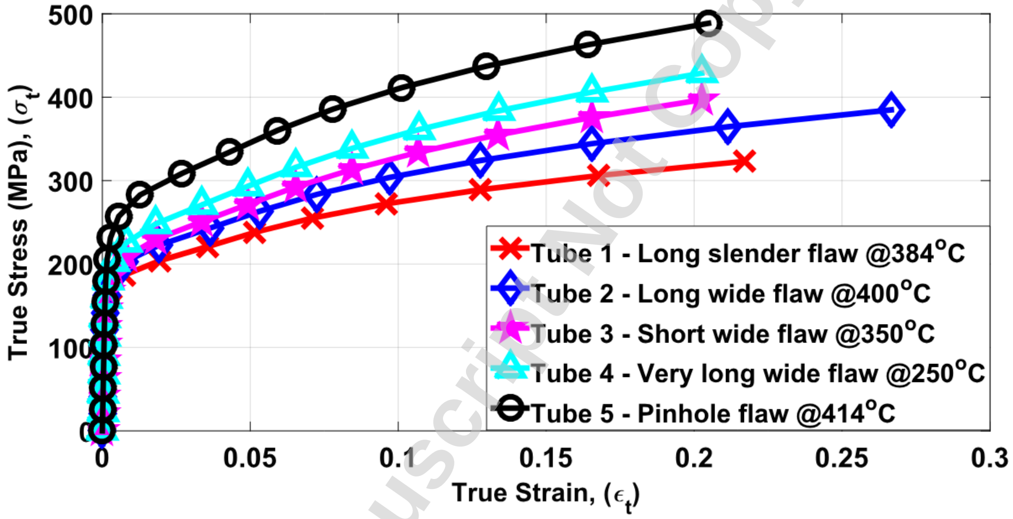

Fig. 7. Material model at the temperatures in which the tubes failed

2.4 *Determination of failure in Finite Element Analysis*

The tube is deemed to have failed when the maximum plastic strain reaches 5%, for which the failure pressure is denoted $P_{5\%}$. This failure criterion is used since it has been shown in previous studies to be an appropriate reference failure limit for pressurized tubes undergoing localization [7,20]. It is also in line with the American Petroleum Institute (API) recommendation of a plastic strain limit at any point in the model [22]. The equivalent plastic strain and von Mises stress distributions for one of the tubes (Tube 2, with a long wide flaw) are shown in Fig. 8. Notice that the tube attains a 5% plastic strain on the pipe' surface at the deepest point of the flaw region, where the wall thickness is at its minimum. At this strain level, the Von-Mises stress reaches approximately 88% of the σ_{uts}, which is within the stress-based limits.

Accepted Manuscript Not Copyedited
Downloaded from http://asmedigitalcollection.asme.org/pressurevesseltech/article-pdf/doi/10.1115/1.4069837/7538655/pvt-24-1191.pdf by University of Pretoria, Ifeanyi Emmanuel Kalu on 21 September 2025

Journal of Pressure Vessel Technology. December 22, 2024;
Accepted manuscript posted September 19, 2025. 10.1115/1.4069837
Copyright (c) 2024 by ASME

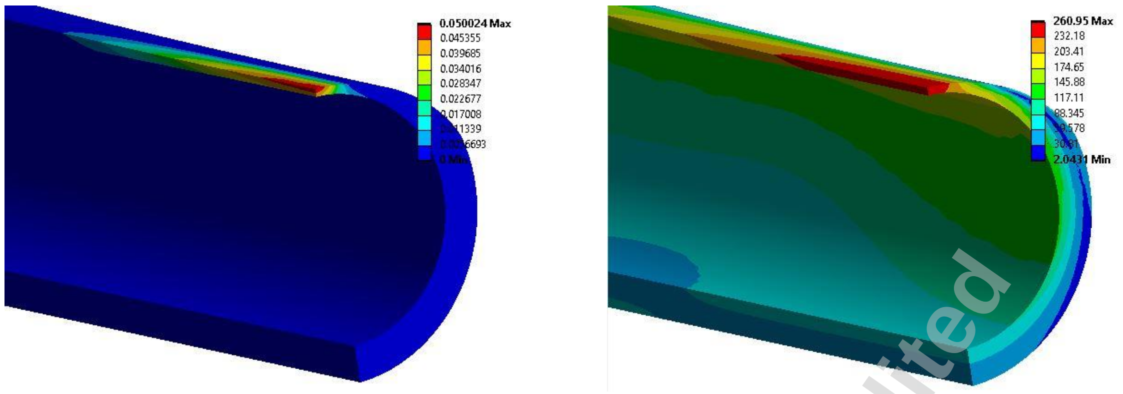

Fig. 8. Equivalent plastic strain and von Mises stress distributions for Tube 2, with a long wide flaw.

3 Comparison between two methods of evolving the flaw dimensions

3.1 Study setup

To identify which geometric parameters are most critical for predicting failure of the tubes and to what extent will they influence their failure, two different modeling methods for evolving flaws to their failure geometry are first compared. The modeling approach (as Case 1) in which the flaw width (f_w) and length (f_l) do not change as the flaw depth (f_d) increases, as was assumed in our previous research [7,19] was compared with an approach in which all the dimensions of the flaw evolve proportionally (as Case 2). This comparison is to check whether the flaw evolution assumption affects the tube failure results. Case 1, illustrated in Fig. 9 (a), maybe conservative (i.e. it predicts a smaller failure pressure) in comparison with Case 2, illustrated in Fig. 9 (b), since there is more material loss at earlier stages of the flaw evolution.

This study includes 50 finite element analyses, representing five different remaining wall thicknesses, t_r, and consequently flaw depths, f_d, for each of the five tubes considered, repeated for both flaw evolution assumptions, shown in Table 3. For each tube, we begin with a known final flaw dimension, (shown by the solid black line in Fig. 9 and create hypothetical smaller flaws with decreasing flaw depth (red lines) up to an assumed initial flaw size (dotted black line). As shown in Table 3, the parametrized flaws can be distinguished by their variation

Accepted Manuscript Not Copyedited
Downloaded from http://asmedigitalcollection.asme.org/pressurevesseltech/article-pdf/doi/10.1115/1.4069837/7538655/pvt-24-1191.pdf by University of Pretoria, Ifeanyi Emmanuel Kalu on 21 September 2025

Journal of Pressure Vessel Technology. December 22, 2024;
Accepted manuscript posted September 19, 2025. 10.1115/1.4069837
Copyright (c) 2024 by ASME

patterns: Case 1 flaws vary in f_d while f_l and f_w remain fixed, whereas Case 2 flaws vary in all dimensions. The f_d/t range is chosen such that the flaws are parameterized from about approximately 40% to about 90% of the initial tube wall thickness, which demonstrates the flaw progression from a point where the tubes will be safe for use to a point where the tubes are known to have failed.

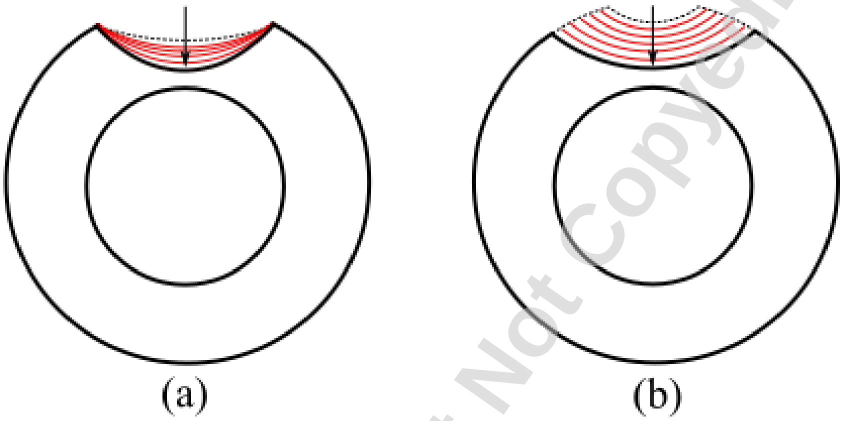

Fig. 9. Cross-section of a flawed tube showing (a) the flaw evolving in depth only (Case 1) and (b) the flaw evolving in all its dimensions (Case 2).

Table 3 Parameterized dimensions of the remodeled flaws

				Case 1		Case 2	
Flaws	t_r (mm)	f_d (mm)	f_d/t	f_l (mm)	f_w (mm)	f_l (mm)	f_w (mm)
Long slender flaw	3.95	3.05	0.44	600	20	411.15	14.62
	2.50	4.50	0.64	600	20	499.19	17.45
	1.50	5.50	0.79	600	20	551.90	18.96
	1.00	6.00	0.86	600	20	576.45	19.51
	0.50	6.50	0.93	600	20	600	20
Long wide flaw	3.27	2.13	0.39	400	45	284.83	38.18
	1.82	3.58	0.66	400	45	369.29	44.11
	1.67	3.73	0.69	400	45	376.95	44.31
	1.44	3.96	0.73	400	45	388.4	44.67
	1.20	4.20	0.78	400	45	400	45
Short wide flaw	3.16	2.24	0.41	310	60	207.85	50.87
	2.30	3.10	0.57	310	60	244.54	55.77
	1.44	3.96	0.73	310	60	276.41	58.76
	0.93	4.47	0.83	310	60	293.68	59.68
	0.42	4.98	0.92	310	60	310	60
Very long wide flaw	2.10	1.70	0.45	500	35	356.17	27.80
	1.55	2.25	0.59	500	35	409.76	30.91
	1.29	2.51	0.66	500	35	432.79	32.11
	0.73	3.07	0.81	500	35	478.64	34.18
	0.45	3.35	0.88	500	35	500	35

Downloaded from http://asmedigitalcollection.asme.org/pressurevesseltech/article-pdf/doi/10.1115/1.4069837/7538655/pvt-24-1191.pdf by University of Pretoria, Ifeanyi Emmanuel Kalu on 21 September 2025
Accepted Manuscript Not Copyedited

Journal of Pressure Vessel Technology. December 22, 2024;
Accepted manuscript posted September 19, 2025. 10.1115/1.4069837
Copyright (c) 2024 by ASME

Pinhole flaw	1.75	1.85	0.51	20	15	14.36	11.24
	1.60	2.00	0.56	20	15	14.97	11.67
	1.10	2.50	0.69	20	15	16.89	12.98
	0.60	3.00	0.83	20	15	18.66	14.15
	0.20	3.40	0.94	20	15	20	15

3.2 Results

For Case 1, in which the flaws evolve only along the depth while other flaw dimensions are fixed, the failure pressure $P_{5\%}$is plotted against the remaining thickness of the flawed tube as it undergoes metal loss, t_r in Fig. 10. The remaining thickness is normalized by the tube thickness to facilitate comparison between different tubes. For Tubes 1 to 4, a linear decrease in failure pressure is observed with increasing flaw depth. It can also be seen that at low remaining tube thickness ratios, t_r/t (where most of the tubes failed), there is a noticeable difference in the tube failure pressure. This is an artefact of the tube remaining thickness at failure, t_{rf}, as flaws were only parametrized up to this value. Given the long dimensions of the flaws in Tubes 1 to 4, failure is assumed to have taken place by rupturing, a failure mechanism attributed to gross plastic deformation of the thinned area resulting in an unstable length-wise propagation of the flaw [26,27].

The conspicuous exception to this is the tube with the pinhole flaw (see Fig. 10), which clearly differs from the failure behavior observed in the other tubes. The failure pressure is approximately double that of the other tubes and the failure pressure decreases nonlinearly with increasing flaw depth. From this model, the tube should still be safe at the operating pressure, giving the high predicted failure pressure. However, in reality this tube failed. This indicates that failure occurred quite early before the flaw developed to a larger size. Unlike other flaws that failed by rupturing, due to the insufficient length of the pinhole flaw to initiate a propagating rupture, the failure mechanism associated with it is most likely a leakage. This is in line with other literature that reported the tendency of small flaws (such as this one) that appear to be like a pinhole or puncture to cause leakages in pipes [26,27]. We argue that for

Downloaded from http://asmedigitalcollection.asme.org/pressurevesseltech/article-pdf/doi/10.1115/1.4069837/7538655/pvt-24-1191.pdf by University of Pretoria, Ifeanyi Emmanuel Kalu on 21 September 2025

Accepted Manuscript Not Copyedited

Journal of Pressure Vessel Technology. December 22, 2024;
Accepted manuscript posted September 19, 2025. 10.1115/1.4069837
Copyright (c) 2024 by ASME

small and localized metal loss flaws plastic collapse is inhibited by the support provided by the surrounding material.

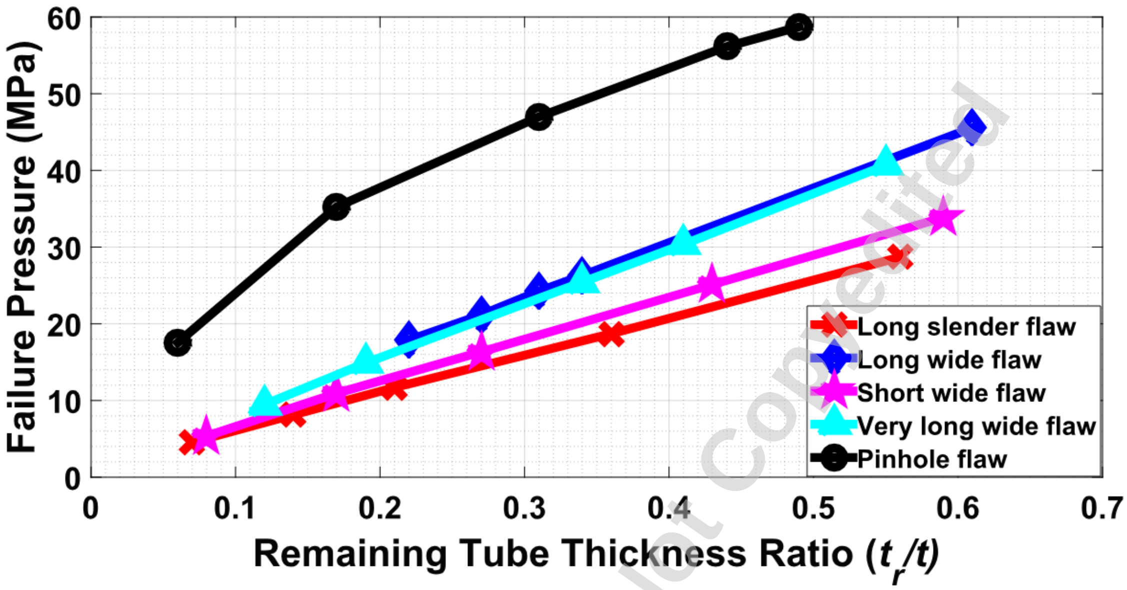

Fig. 10. Failure pressure of Case 1 flawed tubes with respect to their remaining thicknesses.

To check if flaw evolution assumption (such as was employed in Case 1) can affect the tube failure predictions, the results are compared with Case 2, in which flaw progression is modelled in all three dimensions. This will enable us to ascertain whether or not the failure evaluation of in-service metal loss flaws on pressurized tubes is sensitive to how the flaws evolve.

Results for the Case 2 analysis (evolving all flaw dimensions in proportion to each other) are shown in Fig. 11. The same linear relationship is seen again between failure pressures and the ratio of the remaining tube thickness, t_r/t for the flawed tubes, with the exception of the pinhole tube. The two cases are directly compared in Fig. 12, in which the absolute and percentage differences are plotted against the normalized remaining tube thickness, t_r/t. It is noteworthy to report that generally, there is no appreciable difference between the two cases. The difference for Tubes 1 to 4 remains below 2%. Tube 5, containing the pinhole flaw, behaves differently, showing a maximum difference of 7.5%. This can be attributed to the highly localized shape of this flaw, which will result in a substantial difference between the

Accepted Manuscript Not Copyedited
Downloaded from http://asmedigitalcollection.asme.org/pressurevesseltech/article-pdf/doi/10.1115/1.4069837/7538655/pvt-24-1191.pdf by University of Pretoria, Ifeanyi Emmanuel Kalu on 21 September 2025

Journal of Pressure Vessel Technology. December 22, 2024;
Accepted manuscript posted September 19, 2025. 10.1115/1.4069837
Copyright (c) 2024 by ASME

two flaw evolution assumptions. For all flaws, the difference is minimized at the point of minimum remaining thickness, as this represents the same geometry for both cases.

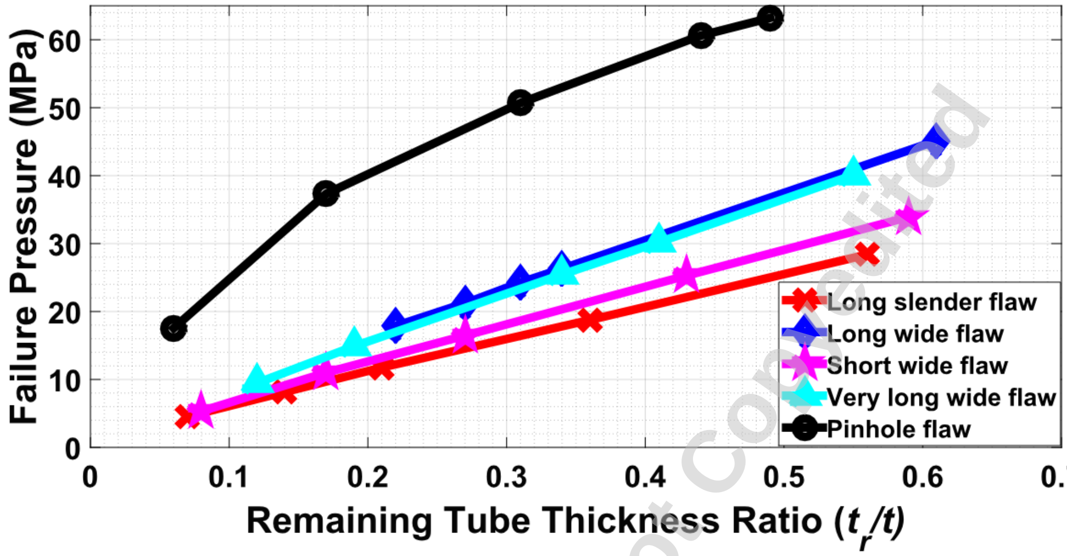

Fig. 11: Failure pressure of Case 2 flaw progression with respect to the remaining tube thicknesses.

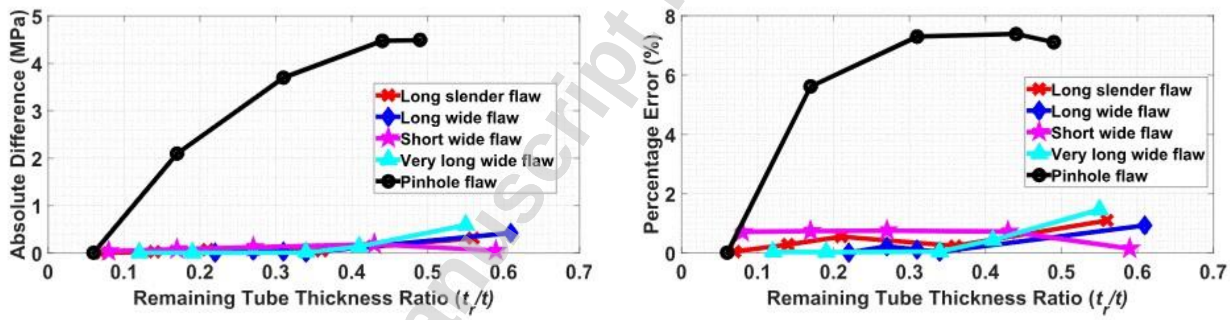

Fig. 12: Absolute and percentage differences between the two case scenarios investigated.

The implication of these results clearly shows that whether a flaw is evolved only by increasing the depth (f_d), while the length (f_l) and width (f_w) remain unchanged, or whether a flaw is evolves in all of its dimensions (f_l, f_w and f_d), the impact on the failure of the tubes will be similar. Thus, changes in localized flaw progression on the tubes will have a negligible effect on their failure. The finding from this investigation using real failed tubes further substantiates previous studies that were done on conceptualized tubes with conservative flaw progression [20,28]. The insight from this analysis shows that failure evaluation of in-service boiler tubes undergoing LML is insensitive to how the flaws evolve. Hence, a convenient method for evolving flaw geometries is sufficient for conducting failure assessment of flawed tubes.

Accepted Manuscript Not Copyedited

Downloaded from http://asmedigitalcollection.asme.org/pressurevesseltech/article-pdf/doi/10.1115/1.4069837/7538655/pvt-24-1191.pdf by University of Pretoria, Ifeanyi Emmanuel Kalu on 21 September 2025

Journal of Pressure Vessel Technology. December 22, 2024;
Accepted manuscript posted September 19, 2025. 10.1115/1.4069837
Copyright (c) 2024 by ASME

4 Effect of the flaw geometry after removing material and tube dimension differences

4.1 Study setup

Although Tube 5 showed a marked difference from the other tubes in the first investigation, it is important to determine whether this was due to the flaw geometry or could it be attributed to the tube material, dimensions and operating conditions. In this investigation, all the flaws are remodeled on the same tube. By so doing, geometry and material factors will be eliminated, thereby giving us a better understanding of the failure mechanism associated with the flaws.

The dimensions (as reported in Table 1) and material properties (as reported in Table 2) of Tube 1 are used as the basis for this study. A hypothetical remaining thickness at failure t_f', is calculated by scaling the original flaw to the new tube thickness. Since the previous study demonstrated that the failure pressure is relatively insensitive to the method of flaw evolution, the flaw lengths and widths remain unscaled. The dimensions of these remodeled flawed tubes are shown in Table 4. The flaws depths are parameterized from about half of their wall thickness to about 90%, to allow for the modeling of the flaws from a safe point (pre-yielding) to the point where they all failed, resulting in 25 finite element analyses.

Table 4. Remodeled tube dimensions

Tubes no	D_o (mm)	t (mm)	t_f' (mm)	f_l (mm)	f_w (mm)	f_d (mm)
1A.	75.0	7.0	0.50	600	20	6.50
2A.	75.0	7.0	1.56	400	45	5.44
3A.	75.0	7.0	0.54	310	60	6.46
4A.	75.0	7.0	0.83	500	35	6.17
5A.	75.0	7.0	0.39	20	15	6.61

4.2 Results

The results are shown in Fig. 13. It is immediately apparent that, with material properties and tube dimensions removed as variables, the results from Tubes 1 to 4 collapse onto a line. Although these flaws range in length from 5 to 13 times the tube diameter, and in width from

Accepted Manuscript Not Copyedited

Downloaded from http://asmedigitalcollection.asme.org/pressurevesseltech/article-pdf/doi/10.1115/1.4069837/7538655/pvt-24-1191.pdf by University of Pretoria, Ifeanyi Emmanuel Kalu on 21 September 2025

Journal of Pressure Vessel Technology. December 22, 2024;
Accepted manuscript posted September 19, 2025. 10.1115/1.4069837
Copyright (c) 2024 by ASME

a quarter of the tube diameter to the full tube diameter, the only component of flaw geometry which impacts the failure pressure is the remaining thickness. In contrast, the difference between the failure pressures associated with the smallest flaw (Tube 5) and those of the other tubes is even more pronounced once the material variation has been removed. This corroborates the inference made earlier from the results in section 3 that Tube 5 failed due to leaking rather than gross plastic collapse. It can also be inferred from the result obtained that as long as the flaws exist under similar tube and material conditions, in spite of their varied geometry, their failure behaviour as they evolve through the tube thickness will be in a similar fashion. Only marginal differences in their failure pressure at the same remaining tube thickness will be seen. This makes the remaining tube thickness a key parameter that can impact tube failure.

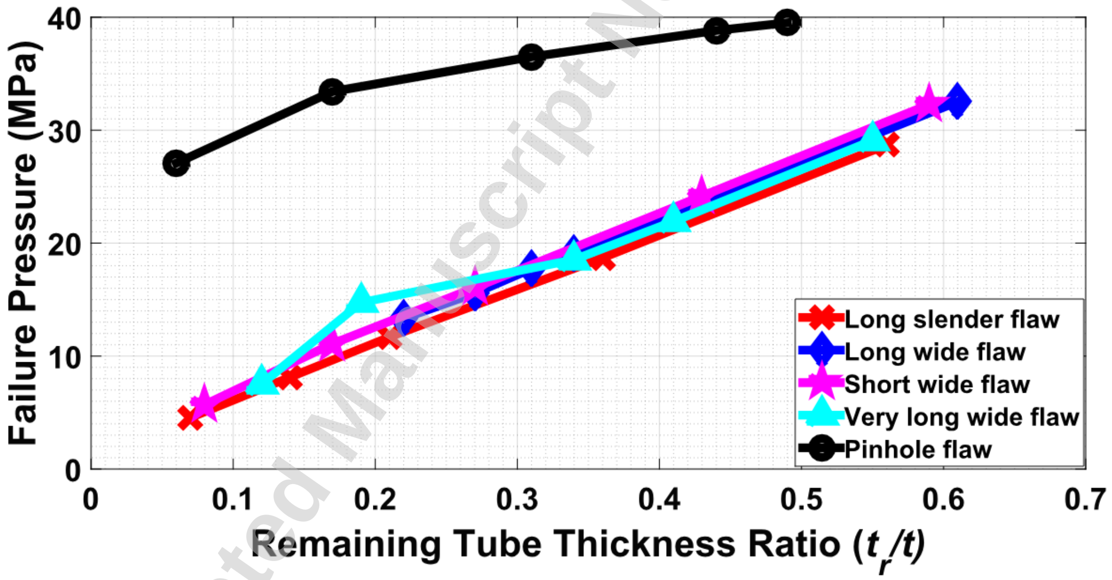

Fig. 13. Failure pressure of the remodeled flawed tube with respect to the remaining tube thickness.

5 Systematic evaluation of flaws spanning a range of sizes

5.1 Study setup

The observed difference in failure pressures between Tube 5 (with the pinhole flaw) and Tubes 1 to 4 (with lengthier and wider flaws) has been attributed to the possibility of a different failure mode – leaking rather than gross plastic collapse. This leads us to investigate flaws which span the space between the pinhole flaw and lengthy flaws to better understand the failure behaviour

Downloaded from http://asmedigitalcollection.asme.org/pressurevesseltech/article-pdf/doi/10.1115/1.4069837/7538655/pvt-24-1191.pdf by University of Pretoria, Ifeanyi Emmanuel Kalu on 21 September 2025

Accepted Manuscript Not Copyedited

Journal of Pressure Vessel Technology. December 22, 2024;
Accepted manuscript posted September 19, 2025. 10.1115/1.4069837
Copyright (c) 2024 by ASME

of the progression of the flaws from a pinhole size to a lengthy size. The study also provides answer to the question of which flaw dimensions is plastic collapse the appropriate failure model. A full-factorial study considering f_l/D_o ratios between 0.267 and 8.0 and f_w/D_o ratios between 0.2 and 0.5 is developed, and illustrated schematically in Fig. 14. These flaws are modeled on Tube 1, with $D_o = 75$ mm and $t = 7$ mm. The specific normalized flaw dimensions are chosen based on the real flaws from Table 1.

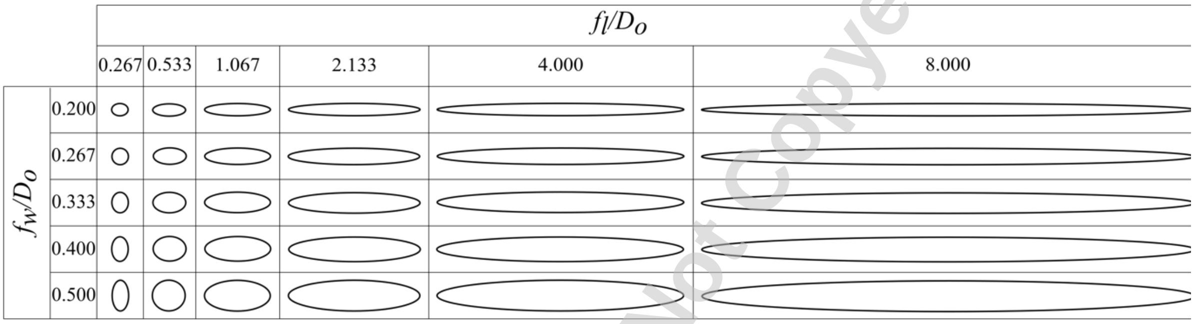

Fig. 14. Pictorial representation of the range of flaw geometries investigated.

For each flaw f_w/D_o ratio, models with each of the f_l/D_o ratios are constructed. Each of the designed flaw models is also parameterized to consider a range of remaining tube thicknesses, t_r, while the f_l/D_o and f_w/D_o of the model remain unchanged. The flaws are parameterized such that t_r varies from about 50% of the initial wall thickness to about 7%, which demonstrates the flaw progression from a point where the flawed tubes are expected to be safe to the point they would have most likely failed. Based on the design set-up, a total of 150 parameterized FE models are constructed and analyzed. Appendix A shows the failure pressure values obtained for each of the 150 FE models that were simulated and analyzed. Fig. 15 shows a representation of the extremes of the simulated flawed tube geometries; with f_l/D_o of 0.267 and 8, combined with f_w/D_o of 0.2 and 0.5. The geometry models of some other f_w/D_o ratios are shown in Appendix B.

Accepted Manuscript Not Copyedited

Downloaded from http://asmedigitalcollection.asme.org/pressurevesseltech/article-pdf/doi/10.1115/1.4069837/7538655/pvt-24-1191.pdf by University of Pretoria, Ifeanyi Emmanuel Kalu on 21 September 2025

Journal of Pressure Vessel Technology. December 22, 2024;
Accepted manuscript posted September 19, 2025. 10.1115/1.4069837
Copyright (c) 2024 by ASME

5.2 Results

Results of the analysis are depicted in Fig. 16 and Fig. 17. Fig. 16 depicts the failure pressure for each flaw width through the different flaw lengths, while Fig. 17 shows the failure pressure results for each flaw length through varied flaw widths considered in this study. In either figure, a similarity in the failure behavior pattern can be seen for all flaws, with the failure pressure generally declining as the t_r/t decreases for most of the flaws. This is consistent with the observation from previous analyses, especially for tubes with the same tube and material condition, as the flaws evolve through the tube thickness.

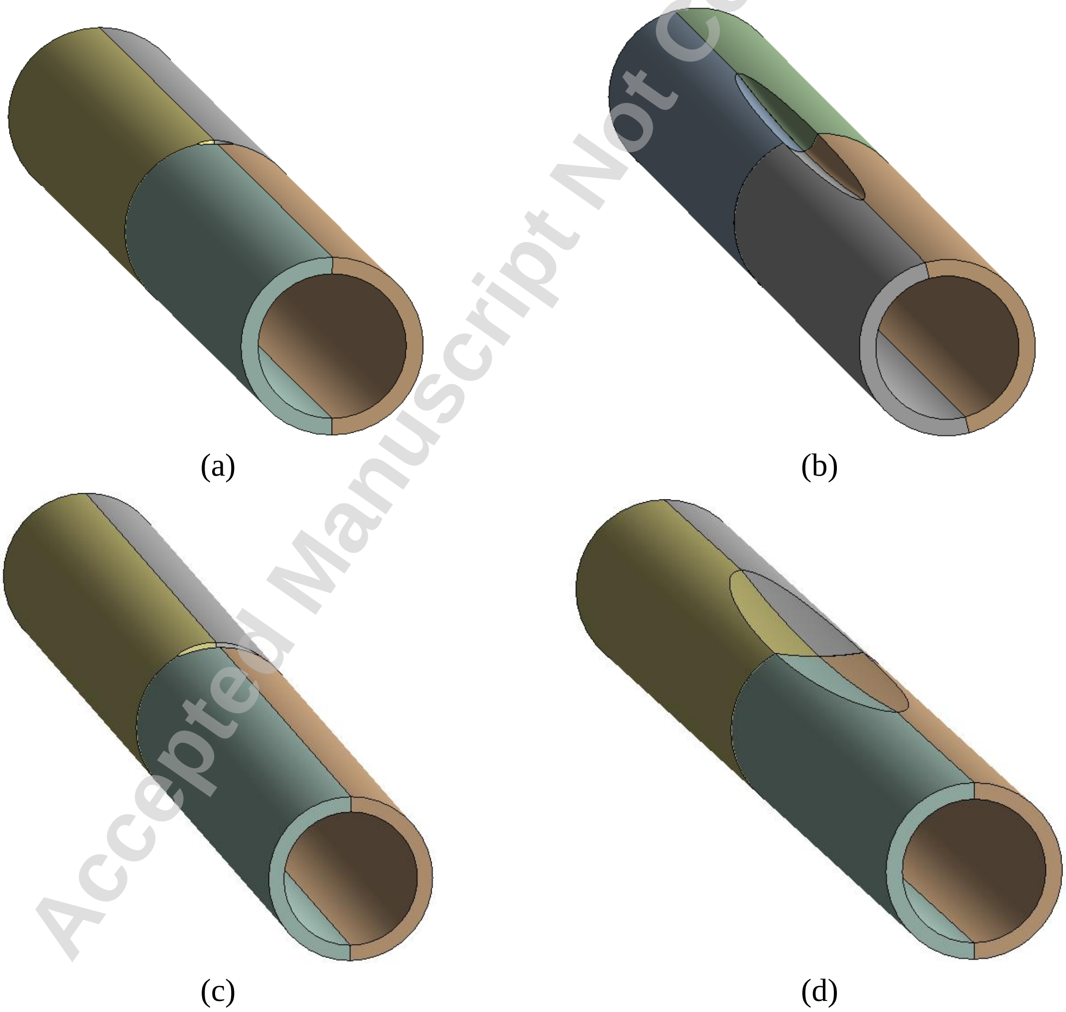

Fig. 15 Simulated flawed tube models for (a) pinhole flaw with $f_l/D_o = 0.267$ and $f_w/D_o = 0.2$ (b) long slender flaw with $f_l/D_o = 8$ and $f_w/D_o = 0.2$ (c) wide pinhole flaw with $f_l/D_o = 0.267$ and $f_w/D_o = 0.5$ (d) long wide flaw with $f_l/D_o = 8$ and $f_w/D_o = 0.5$.

In Fig. 16 the failure pressure is plotted against the normalized flaw lengths for a range of remaining thicknesses (shown as different lines on each graph) for increasing normalized flaw

Downloaded from http://asmedigitalcollection.asme.org/pressurevesseltech/article-pdf/doi/10.1115/1.4069837/7538655/pvt-24-1191.pdf by University of Pretoria, Ifeanyi Emmanuel Kalu on 21 September 2025

Accepted Manuscript Not Copyedited

Journal of Pressure Vessel Technology. December 22, 2024;
Accepted manuscript posted September 19, 2025. 10.1115/1.4069837
Copyright (c) 2024 by ASME

widths in subfigures (a) to (e). The curves all show the same trend, with a steep initial slope for small lengths, decreasing as the length increases. From $f_l/D_o \sim 2$ the curve begins to flatten and variation in the failure pressure diminishes. After this point, no appreciable difference in failure pressure is seen for longer flaws. This point can be taken as a transition point between short and sufficiently long flaws.

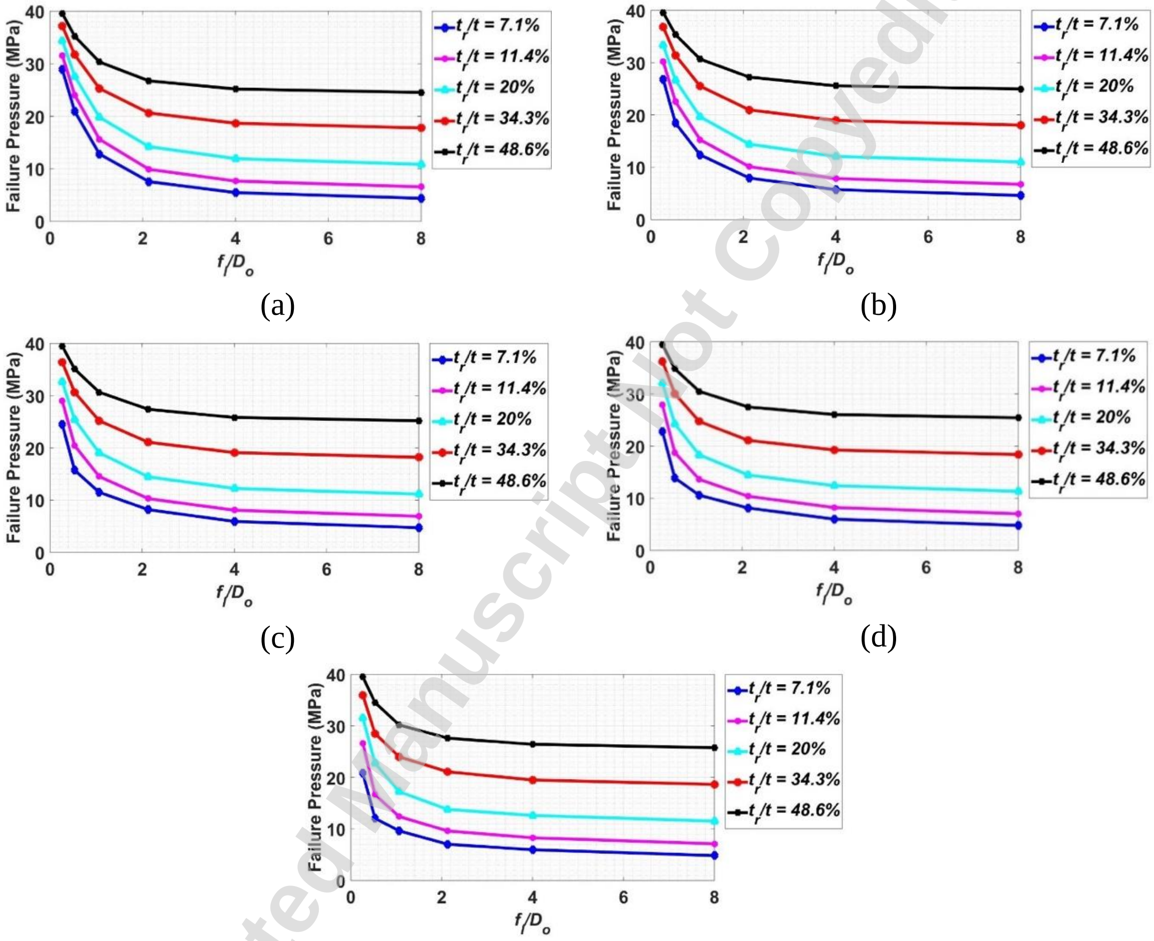

Fig. 16. Failure analysis results for simulated flaws through increasing flaw length (f_l/D_o) for different flaw widths (a) $f_w/D_o = 0.2$ (b) $f_w/D_o = 0.267$ (c) $f_w/D_o = 0.333$ (d) $f_w/D_o = 0.4$ (e) $f_w/D_o = 0.5$

For short flaws, the predicted failure pressure is strongly inversely related to the flaw length. This decrease in failure pressure associated with the flaw length is only observable up to the transition point ($f_l/D_o \sim 2$), after which the curve tends to an asymptote. For flaws longer than this transition ratio ($f_l/D_o > 2$) the failure pressure does not depend on the flaw length, allowing for an appropriate estimation of the failure pressure of long flaws irrespective of their width.

Accepted Manuscript Not Copyedited

Downloaded from http://asmedigitalcollection.asme.org/pressurevesseltech/article-pdf/doi/10.1115/1.4069837/7538655/pvt-24-1191.pdf by University of Pretoria, Ifeanyi Emmanuel Kalu on 21 September 2025

Journal of Pressure Vessel Technology. December 22, 2024;
Accepted manuscript posted September 19, 2025. 10.1115/1.4069837
Copyright (c) 2024 by ASME

This outcome on pressurized tubes with LML flaws correlates with studies on defected pipes that showed explicit limits for lengthy flaws, which allows for their failure pressure estimations, while providing a specific burst pressure expression for finite flaw sizes [29,30].

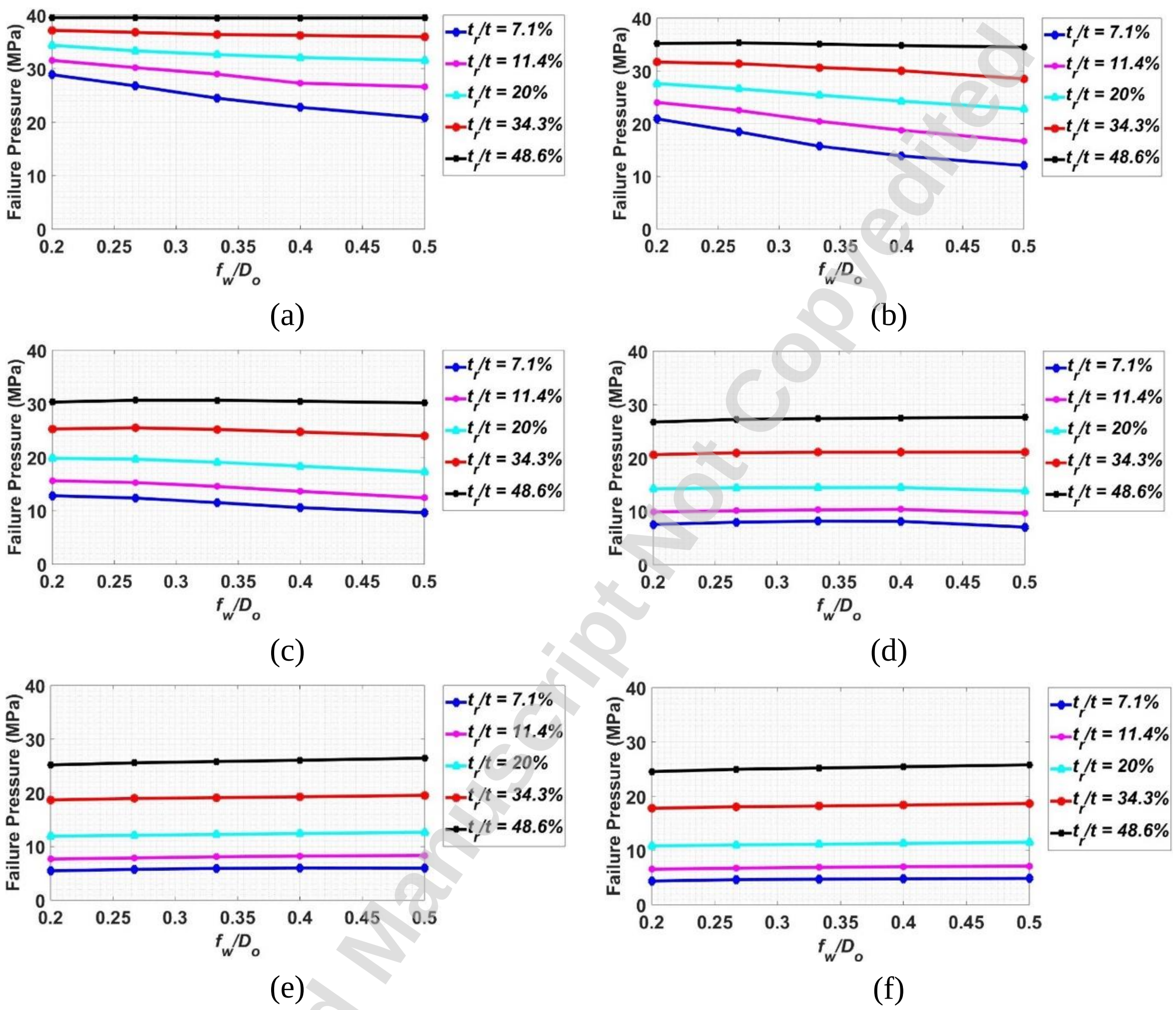

Fig. 17. Failure analysis results for simulated flaws through increasing flaw width (f_w/D_o) for different flaw lengths (a) $f_l/D_o = 0.267$ (b) $f_l/D_o = 0.533$ (c) $f_l/D_o = 1.067$ (d) $f_l/D_o = 2.133$ (e) $f_l\,/D_o = 4$. (f) $f_l/D_o = 8$.

In Fig. 17, the failure pressure is plotted against the normalized flaw widths for a range of remaining thicknesses (shown as different lines on each graph) for increasing normalized flaw lengths in subfigures (a) to (f). As can be observed, the failure pressure generally decreases for decreasing remaining thickness. For flaw length ratios up to $f_l/D_o = 1.067$, the failure pressure shows a slight linear decrease as the flaw width increases, and a pronounced decrease between different flaw length graphs. For flaw length ratios of $f_l/D_o = 2.133$ and higher, the

Downloaded from http://asmedigitalcollection.asme.org/pressurevesseltech/article-pdf/doi/10.1115/1.4069837/7538655/pvt-24-1191.pdf by University of Pretoria, Ifeanyi Emmanuel Kalu on 21 September 2025
Accepted Manuscript Not Copyedited

Journal of Pressure Vessel Technology. December 22, 2024;
Accepted manuscript posted September 19, 2025. 10.1115/1.4069837
Copyright (c) 2024 by ASME

results are constant for both flaw width and flaw depth. As such, the contributory influence of the flaw width towards the tube failure is only pronounced for small flaw lengths ($f_l/D_o \leq 1$).

The result obtained from this study demonstrates that short flaws with lengths $f_l/D_o < 2$ are increasingly sensitive to the flaw geometry as the length and width decrease. As such, careful attention should to be given to such flaws during maintenance schedules. It is expected that deep flaws of small width and length will fail by a mechanism such as leaking rather than by gross plastic collapse. More so, this study by implication establishes the limits of validity of our previously proposed failure prediction methodology in [7,19]. It is recommend that the failure methodology should not be used for flaws with a length shorter than twice the pipe diameter, as these flaws are not well characterized by gross plastic collapse. In contrast, for flaw lengths of $f_l/D_o \geq 2$, the failure pressure shows no sensitivity to flaw width or depth, and is solely governed by the remaining flaw thickness, enabling efficient estimation of failure pressure and risk-based prioritization for in-service integrity assessments of pressurized tubes.

6 Conclusions

In this paper, comprehensive investigative studies were carried out on various metal loss flaws to acquire insights on their failure behaviour and mechanism, especially as they progress from very small size to lengthy. Flawed tubes with different aspect ratios and descriptions (long slender, long wide, short wide, very long wide and pinhole flaws) that cover a variety of localized metal loss (LML) scenarios were analyzed. A total of 225 finite element analyses were conducted in this study. The following findings were made:

1. The assessment of most in-service metal loss flaws on pressurized tubes is insensitive to how the flaws evolve to failure. As such, any convenient geometry that can reasonably characterize the progression of the flaw will be adequate for conducting the failure analysis of in-service tubes with LML.

Accepted Manuscript Not Copyedited

Downloaded from http://asmedigitalcollection.asme.org/pressurevesseltech/article-pdf/doi/10.1115/1.4069837/7538655/pvt-24-1191.pdf by University of Pretoria, Ifeanyi Emmanuel Kalu on 21 September 2025

Journal of Pressure Vessel Technology. December 22, 2024;
Accepted manuscript posted September 19, 2025. 10.1115/1.4069837
Copyright (c) 2024 by ASME

2. For sufficiently large flaws which can be expected to fail by rupture following gross plastic collapse, a linear relationship exists between the failure pressure of flawed tubes and the remaining thickness at the flaw's deepest point.
3. A notable exception to this failure pattern is seen with small deep flaws, which are postulated to fail by leaking rather than by plastic collapse, since plastic collapse is inhibited by the support provided by the surrounding material.
4. As long as flaws exist under similar tube and material conditions, in spite of their varied geometries, their failure behavior as they evolve through their wall thicknesses will be in a similar fashion. Only marginal differences in their failure pressure at the same remaining tube thickness will be seen.
5. Failure pressure for small flaws is very sensitive to their flaw geometries and is not adequately characterized by gross plastic collapse. The apparent decrease in failure pressure of the deep finite size flaws due to the effect of the small flaw length and width warrants that more careful attention must be given to such flaws in practice.
6. The failure pressure ceases to depend on the flaw length when it is greater than twice the tube diameter, and ceases to depend on the flaw width when the flaw length is greater than the tube diameter. Once the flaw length is at least twice the tube diameter, the only flaw dimension which is necessary to predict failure is the remaining tube thickness in the deepest part of the flaw.
7. The findings from this research establishes the applicability limits of gross plastic collapse analysis for pressurized tubes experiencing metal loss. It also substantiates the validity of our previously proposed failure prediction methodology for conducting fitness for service assessment on metal loss flaws in a high pressure and high temperature environment.

Accepted Manuscript Not Copyedited

Downloaded from http://asmedigitalcollection.asme.org/pressurevesseltech/article-pdf/doi/10.1115/1.4069837/7538655/pvt-24-1191.pdf by University of Pretoria, Ifeanyi Emmanuel Kalu on 21 September 2025

Journal of Pressure Vessel Technology. December 22, 2024;
Accepted manuscript posted September 19, 2025. 10.1115/1.4069837
Copyright (c) 2024 by ASME

All the outcomes from this study helped us to better understand the failure behavioral pattern and mechanisms associated with localized metal loss flaws of varying sizes. The insights from this work will be useful for the maintenance of these pressurized tubes while in service.

Acknowledgements

The authors express gratitude to the University of Pretoria Department of Research and Innovation for the financial support provided for this Postdoctoral research study.

References

[1] A. Saha, H. Roy, Failure investigation of a secondary super heater tube in a 140 MW thermal power plant, Case Stud. Eng. Fail. Anal. 8 (2017) 57–60. https://doi.org/10.1016/j.csefa.2017.05.001.

[2] J. Roy-Aikins, Challenges in meeting the electricity needs of South Africa, in: Proc. ASME 2016 Power Energy Conf., 2016: p. V001T05A002.

[3] R. Viswanathan, Life management of high-temperature piping and tubing in fossil power plants, J. Press. Vessel Technol. Trans. ASME. 122 (2000) 305–316. https://doi.org/10.1115/1.556187.

[4] Electric Power Research Institute (EPRI), Guidelines for control and prevention of fly ash erosion, CA, USA, 2011.

[5] I. Klevtsov, H. Tallermo, T. Bojarinova, A. Dedov, Assessment of remaining life of superheater austenitic steel tubes in oil shale PF boilers, Oil Shale. 23 (2006) 267–274.

[6] K. Zarrabi, Estimation of boiler tube life in presence of corrosion and erosion processes, Int. J. Press. Vessel. Pip. 53 (1993) 351–358.

[7] I.E. Kalu, H.M. Inglis, S. Kok, Prediction of the Time to Failure of Boiler Tubes Flawed With Localized Erosion, J. Press. Vessel Technol. 145 (2023) 1–9. https://doi.org/10.1115/1.4056606.

[8] J. Kim, Y. Kim, B. Kang, S. Hwang, Finite element analysis for bursting failure prediction in bulge forming of a seamed tube, Finite Elem. Anal. Des. 40 (2004) 953–966.

[9] K. Zarrabi, H. Zhang, Creep and plastic collapse lives of scarred boiler tubes, Mater. High Temp. 15 (1998) 389–393.

[10] K. Zarrabi, Plastic collapse pressures for defected cylindrical vessels, Int. J. Press. Vessel. Pip. 60 (1994) 65–69.

[11] M. Suckling, C. Allen, Critical variables in high temperature erosive wear, Wear. 203–204 (1997) 528–536.

[12] J.R. Sims, B.F. Hantz, K.E. Kuehn, A basis for the fitness for service evaluation, Press. Vessel Fract. Fatigue, Life Manag. ASME PVP. 233 (1992) 51–58.

[13] B.F. Hantz, J.R. Sims, C.T. Kenyon, T.A. Turbak, Fitness for service: Groove-like local thin-areas on pressure vessels and storage tanks, Plant Syst. Aging Manag. ASME PVP. 252 (1993) 113–120.

[14] T.A. DePadova, J.R. Sims, Fitness for Service - Local thin areas comparison of finite element analysis to physical test results, Fitness-for-Service Decis. Pet. Chem. Equipment, ASME PVP.

Accepted Manuscript Not Copyedited

Downloaded from http://asmedigitalcollection.asme.org/pressurevesseltech/article-pdf/doi/10.1115/1.4069837/7538655/pvt-24-1191.pdf by University of Pretoria, Ifeanyi Emmanuel Kalu on 21 September 2025

Journal of Pressure Vessel Technology. December 22, 2024;
Accepted manuscript posted September 19, 2025. 10.1115/1.4069837
Copyright (c) 2024 by ASME

315 (1995) 285–292.

[15] D.-J. Shim, J. Choi, Y. Kim, Failure strength assessment of pipes with local wall thinning under combined loading based on finite element analyses, J. Press. Vesssel Technol. 126 (2004) 179–183.

[16] D.-J. Shim, Y.-J.Y.-J. Kim, Y.-J.Y.-J. Kim, Reference stress based approach to predict failure strength of pipes with local wall thinning under combined loading, Trans. ASME. 127 (2005) 76–83. https://doi.org/10.1115/1.1849228.

[17] G. Fekete, L. Varga, The effect of the width to length ratios of corrosion defects on the burst pressures of transmission pipelines, Eng. Fail. Anal. 21 (2012) 21–30.

[18] Y. Gong, Z. Yang, J. Yuan, Failure analysis of leakage on titanium tubes within heat exchangers in a nuclear power plant. Part II : Mechanical degradation, Mater. Corros. 63 (2012) 18–28.

[19] I.E. Kalu, H.M. Inglis, S. Kok, Failure assessment methodology for boiler tubes with localized external erosion defects, Int. J. Press. Vessel. Pip. 188 (2020) 1–18. https://doi.org/10.1016/j.ijpvp.2020.104190.

[20] I.E. Kalu, H.M. Inglis, S. Kok, The sensitivity of failure analysis of boiler tubes to the shape of elliptical external erosion flaws, Eng. Fail. Anal. 119 (2021) 1–16. https://doi.org/10.1016/j.engfailanal.2020.104952.

[21] American Petroleum Institute (API) and the American Society of Mechanical Engineers (ASME), Fitness-For-Service API 579-1/ASME FFS-1, Washinghton, D.C., USA, 2016.

[22] American Petroleum Institute (API), API 579 Recommended practice for Fitness-For-Service, 2000.

[23] Y. Lu, C. Wang, Effects of thickness profile and inner/outer of localized thin area defects on the remaining strength of pressure equipment, J. Loss Prev. Process Ind. 84 (2023) 1–11. https://doi.org/10.1016/j.jlp.2023.105132.

[24] British Standards Institution (BSI), BS 3059: Part 2:1990 British Standard on Steel boiler and superheater tubes, 1990.

[25] M. Kamaya, Stress – strain curve estimation procedures for stainless steels based on yield and ultimate strengths, 127 (2014) 194–210. https://doi.org/10.1016/j.engfracmech.2014.06.008.

[26] H.M. Al-muslim, M.J. Rosenfeld, Leak vs. Rupture Thresholds for Material and Construction Anomalies, 2013.

[27] H. Wang, I.J. Duncan, Likelihood, causes , and consequences of focused leakage and rupture of U . S . natural gas transmission pipelines, J. Loss Prev. Process Ind. 30 (2014) 177–187. https://doi.org/10.1016/j.jlp.2014.05.009.

[28] I.E. Kalu, H.M. Inglis, S. Kok, Effect of defect geometry of localized external erosion on failure of boiler tubes, in: Proc. ASME 2018 Press. Vessel. Pip. Conf. Vol. 3B Des. Anal., Prague, Czech Republic, 2018: p. V03BT03A037. https://doi.org/https://doi.org/10.1115/PVP2018-84787.

[29] T.A. Netto, U.S. Ferraz, S.F. Estefen, On the effect of corrosion defects on the collapse pressure of pipelines, J. Constr. Steel Res. 61 (2005) 1185–1204. https://doi.org/10.1016/j.ijsolstr.2007.04.028.

[30] Y. Shuai, J. Shuai, K. Xu, Probabilistic analysis of corroded pipelines based on a new failure pressure model, Eng. Fail. Anal. 81 (2017) 216–233. https://doi.org/10.1016/j.engfailanal.2017.06.050.

Accepted Manuscript Not Copyedited

Downloaded from http://asmedigitalcollection.asme.org/pressurevesseltech/article-pdf/doi/10.1115/1.4069837/7538655/pvt-24-1191.pdf by University of Pretoria, Ifeanyi Emmanuel Kalu on 21 September 2025

Journal of Pressure Vessel Technology. December 22, 2024;
Accepted manuscript posted September 19, 2025. 10.1115/1.4069837
Copyright (c) 2024 by ASME

Appendix A

Failure pressures for all the simulated FE models constructed from the pinhole size to the long flaw wide flaw at varying remaining thicknesses.

Table A1 Failure pressure for each flaw at the given remaining thickness

	t_r/t (%)	7.1	11.4	20.0	34.3	48.6
f_w/D_o	f_l/D_o			Failure pressure [MPa]		
0.200	0.267	28.884	31.561	34.386	37.176	39.551
	0.533	20.911	24.030	27.594	31.689	35.215
	1.067	12.807	15.611	19.820	25.278	30.328
	2.133	7.554	9.899	14.206	20.617	26.734
	4.000	5.466	7.661	11.930	18.668	25.184
	8.000	4.380	6.560	10.844	17.762	24.531
0.267	0.267	26.790	30.207	33.349	36.787	39.555
	0.533	18.435	22.518	26.618	31.395	35.336
	1.067	12.382	15.275	19.651	25.494	30.663
	2.133	7.953	10.112	14.417	20.969	27.224
	4.000	5.746	7.865	12.089	18.946	25.571
	8.000	4.622	6.751	11.015	18.060	24.963
0.333	0.267	24.487	28.975	32.647	36.396	39.480
	0.533	15.727	20.451	25.427	30.650	35.089
	1.067	11.502	14.527	19.068	25.197	30.657
	2.133	8.170	10.279	14.446	21.073	27.384
	4.000	5.917	8.068	12.235	19.088	25.815
	8.000	4.724	6.904	11.152	18.190	25.185
0.400	0.267	22.779	27.292	32.096	36.233	39.476
	0.533	13.894	18.766	24.272	30.051	34.827
	1.067	10.581	13.622	18.325	24.720	30.485
	2.133	8.122	10.373	14.453	21.089	27.496
	4.000	6.003	8.221	12.415	19.250	26.043
	8.000	4.791	7.016	11.315	18.364	25.428
0.500	0.267	20.818	26.620	31.549	35.980	39.509
	0.533	12.064	16.650	22.769	28.519	34.537
	1.067	9.640	12.407	17.240	24.006	30.183
	2.133	7.047	9.624	13.806	21.106	27.633
	4.000	5.979	8.301	12.639	19.518	26.437
	8.000	4.849	7.130	11.528	18.655	25.779

Accepted Manuscript Not Copyedited

Downloaded from http://asmedigitalcollection.asme.org/pressurevesseltech/article-pdf/doi/10.1115/1.4069837/7538655/pvt-24-1191.pdf by University of Pretoria, Ifeanyi Emmanuel Kalu on 21 September 2025

Journal of Pressure Vessel Technology. December 22, 2024;
Accepted manuscript posted September 19, 2025. 10.1115/1.4069837
Copyright (c) 2024 by ASME

Appendix B

Geometry of additional simulated pinhole flaw size and most lengthy flaw size models.

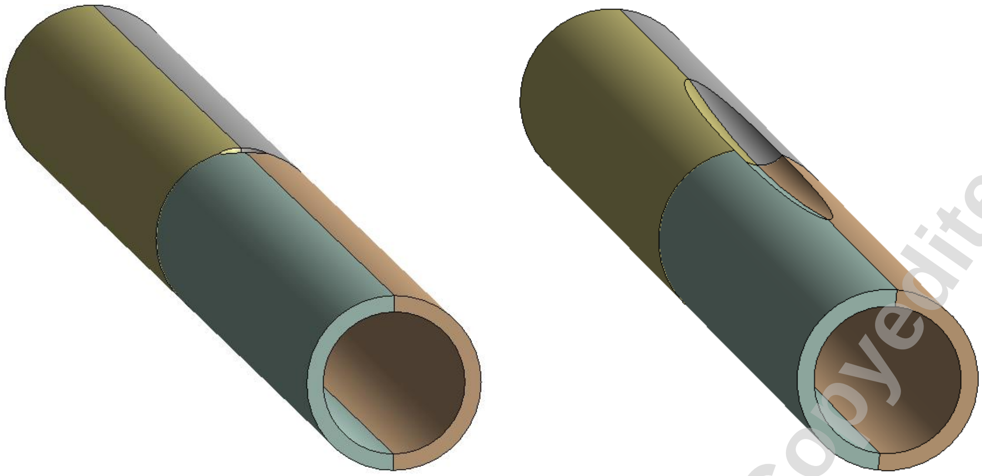

…………………………. (a)……………………………………………… (b)

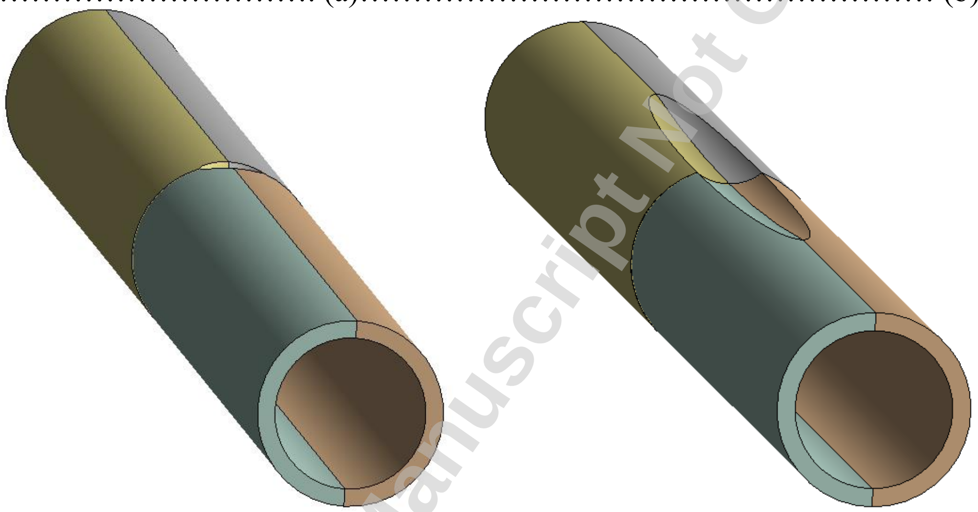

…………………………... (c)…………………………………………….... (d)

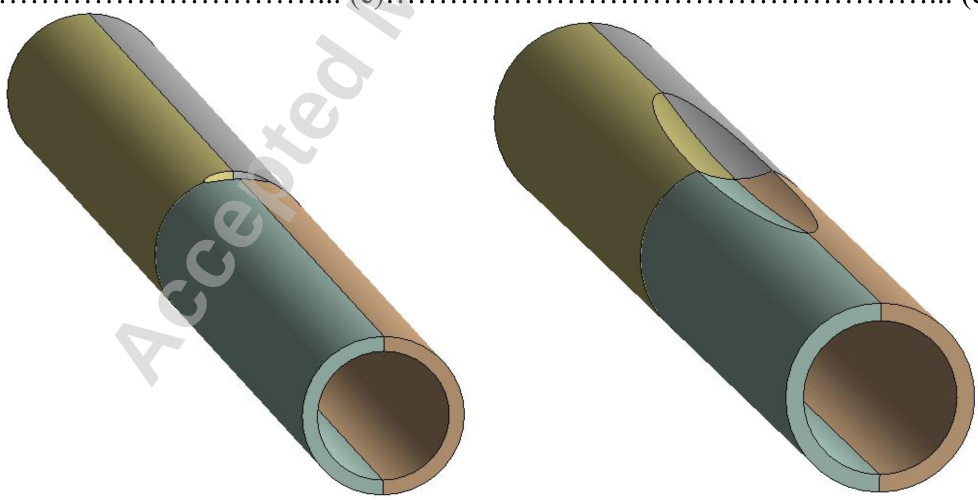

………………………….. (e)……………………………………......... (f)

Fig. B 1. Simulated flawed tube models for (a) pinhole size flaw with $f_l/D_o = 0.267$ and $f_w/D_o = 0.267$ (b) lengthy size flaw with $f_l/D_o = 8$ and $f_w/D_o = 0.267$ (c) pinhole size flaw with $f_l/D_o = 0.267$ and 0.333 (d) lengthy size flaw with$f_l/D_o = 8$ and $f_w/D_o = 0.333$ (e) pinhole size flaw with $f_l/D_o = 0.267$ and 0.4 (f) lengthy size flaw with $f_l/D_o = 8$ and $f_w/D_o = 0.4$.

Accepted Manuscript Not Copyedited

Downloaded from http://asmedigitalcollection.asme.org/pressurevesseltech/article-pdf/doi/10.1115/1.4069837/7538655/pvt-24-1191.pdf by University of Pretoria, Ifeanyi Emmanuel Kalu on 21 September 2025